ISIJ International, Vol. 43 (2003), No. 3, pp. 410–419

The Nature and Consequences of Coherent Transformations in Steel

J. W. MORRIS, Jr., C. S. LEE and Z. GUO

Department of Materials Science and Engineering, University of California, Berkeley, CA 94720 USA.

(*Received on July 10, 2002; accepted in final form on November 6, 2002*)

Advanced research on structural steels has recently focused on the improvement of properties through the control of grain size. Grain refinement increases strength *via* the Hall–Petch relation, lowers the ductile–brittle transition by increasing resistance to transgranular cleavage, and reduces hydrogen embrittlement by minimizing interfacial fracture along grain or lath boundaries. However, given their different mechanisms, these properties require slightly different measures of the effective grain size. When the grains are smooth and random, all measures of the effective grain size are roughly equivalent. However, transformations in steel are often crystallographically coherent, producing a martensitic, bainitic or ferritic product that has either a Kurdumov–Sachs (KS) or a Nishiyama–Wasserman (NW) relation to the parent austenite. The 24 KS variants and 12 NW variants divide into three sets of eight, corresponding to the three Bain variants of the fcc→bcc transformation. Grain, packet or block boundaries that separate different Bain variants have significant misorientations of the {100} cleavage planes, but may have only slight misorientations of the {110} slip planes. It follows that grain refinement through coherent transformation is very effective in improving resistance to cleavage fracture and, if the boundary facets are small, to hydrogen embrittlement, but is often relatively ineffective in increasing strength. For this reason, grain refinement for increased strength is best done with incoherent transformations (such as the strain-induced ferrite transformation) while grain refinement for low-temperature toughness or hydrogen resistance is best done with coherent transformations that refine the effective grain size without overstrengthening to unacceptably low ductility.

KEY WORDS: grain refinement; coherent transformations; strength; ductile–brittle transition; hydrogen embrittlement.

1. Introduction

It is well known that the mechanical properties of ferritic or martensitic steels improve as the grain size is refined. This principle is the basis for many of the thermal and thermomechanical processes used in the making of steel, and is the specific principle used in current research toward "supersteels" that combine excellent strength, toughness and hydrogen resistance at low cost.[1–4)]

On the other hand, it is not entirely clear what is meant by "grain size", or how it should be measured, particularly when adjacent grains are not entirely independent in their crystallography.[5)] A classic example is the effective grain size of lath martensitic steels, in which optical or bright-field TEM measures of the apparent grain size can be frankly deceptive; the microstructure is divided into packets or blocks of similarly oriented martensite laths that behave, in most respects, as single grains.[6–10)] This happens because the transformation is crystallographically coherent. The martensite product has a well-defined crystallographic correspondence with the austenite parent. Crystallographic coherence limits the extent to which a martensitic transformation can refine the microstructure.

While the crystallographic coherence of martensitic transformations is well known, recent research[11–18)] has shown that other mechanisms of the $\gamma \rightarrow \alpha$ transformation, including diffusional mechanisms, are often coherent as well. It is, therefore, important to understand the implications of coherent transformations for grain refinement. We examine this question in the present paper.

We shall specifically consider three properties that are often critical to the performance of structural steels: the strength, the ductile–brittle transition temperature (T_B) and the susceptibility to hydrogen embrittlement. Each of these is strongly affected by grain size. However, the appropriate measure of grain size is different in each case. We next give a brief review of the crystallography of coherent transformations. We then consider how coherent transformations influence the appropriate measure of grain size for each of the three properties of interest. The results of this investigation suggest why coherent transformations are often particularly useful in refining the grain size to resist cleavage fracture or hydrogen embrittlement, but are less effective than incoherent transformations in increasing alloy strength.

2. The Meaning of Grain Size

2.1. The Classic Hall–Petch Relations

It is well known that the strength, cleavage resistance,

and ductile–brittle transition temperature of structural steels obey relations of the Hall–Petch form. The yield strength is given by the classic Hall–Petch relation:

$$\sigma_y = \sigma_0 + K_y d^{-1/2} \quad \text{.....(1)}$$

where d is the mean grain size and K_y is the Hall–Petch coefficient for strength. The cleavage fracture stress obeys a relation of the form

$$\sigma_f = K_f d^{-1/2} \quad \text{.....(2)}$$

where K_f is the Hall–Petch coefficient for cleavage. The ductile–brittle transition temperature often obeys a constitutive equation of the form

$$T_B = T_0 - K_B d^{-1/2} \quad \text{.....(3)}$$

where K_B is the appropriate Hall–Petch coefficient. While the same parameter, the grain size, d, appears in each of these equations, it is important to recognize that "grain size" has a different meaning for each of the properties of interest.

2.2. The Effective Grain Size for Strength

As we have discussed elsewhere,[5] several different theories have been advanced to explain the Hall–Petch relation for strength. Without taking a firm position with respect to these, they have the common feature that grain size limits the distance over which free slip can occur. In Fe, the primary slip planes are the {110} planes, so slip is limited by the dimension of the {110} planes within a grain. Hence the appropriate measure of grain size would appear to be the coherence length along {110}.

The dependence of the Hall–Petch coefficient, K_y, on the properties of the steel are also at least qualitatively common to the various theories. For example, the classic "pile-up" model of the Hall–Petch relation gives

$$K_y \sim 3\left[\frac{2Gb\tau_b}{q\pi}\right]^{1/2} \quad \text{.....(4)}$$

where we have approximated the yield strength by the usual relation, $\sigma_y \sim 3\tau_c$, with τ_c the critical resolved shear stress. In this equation, q is a geometric factor of order unity, G is the shear modulus, b the Burgers vector, and τ_b is the critical shear stress for the transmission of slip across a grain boundary.

If we examine Eq. (4) from the perspective of the controllability of the Hall–Petch coefficient, the Burgers vector is fixed by the crystal and the shear modulus can only be changed by significantly changing the composition of the steel. The variable parameter is τ_b. This parameter is affected by the nature of the grain boundary. It is expected to increase with the misorientation of the dominant ⟨110⟩ slip planes. Increasing the typical misorientation should increase τ_b, hence K_y, while decreasing misorientation should decrease K_y. To maximize the strengthening that can be accomplished by grain refinement, K_y should be as large as possible.

There is, however, a constraint on the useful strength that can be realized through grain refinement.[19–21] For typical steels, the Hall–Petch slope for the ultimate strength is less than that for the yield strength, with the consequence that there is a significant loss of ductility at fine grain size. While recent results suggest that it may be possible to maintain useful ductility in ultrafine-grained dual-phase steels,[22,23] the possible tensile ductility is a serious concern for steels with grain size below about 2 μm.

2.3. The Effective Grain Size for Cleavage and the Brittle Transition

Since iron cleaves on {100} planes, the appropriate measure of grain size for cleavage should be the coherence length on {100}. The Hall–Petch coefficient for cleavage fracture, K_f, should increase with the misorientation of {100} planes across the boundaries.

In many steels, particularly martensitic steels, this coherence length is subtle and difficult to measure.[6,8] For example, **Fig. 1** shows the visual microstructure of a typical lath martensitic steel. A prior austenite grain contains a very large number of discrete laths of dislocated martensite. These are organized into packets, in which the laths share the same habit plane, and packets are often subdivided into blocks in which the parallel laths are the same crystallographic variant of the martensitic transformation.

In optical micrographs, and even in bright-field TEM (**Fig. 2**) the microstructure appears to be highly refined. However, appearances can be deceptive. Figure 2 also con-

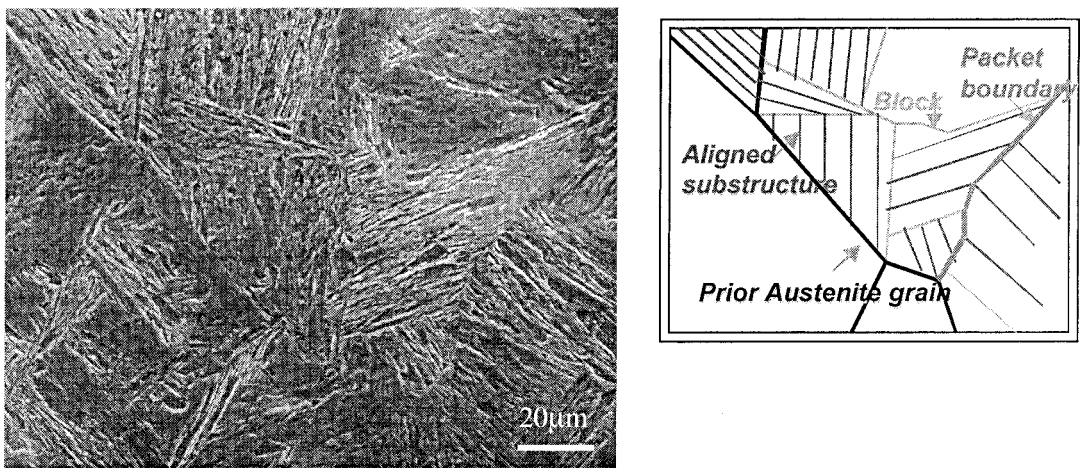

Fig. 1. Scanning electron micrograph of lath martensitic steel showing thin laths of martensite aligned into blocks and packets.

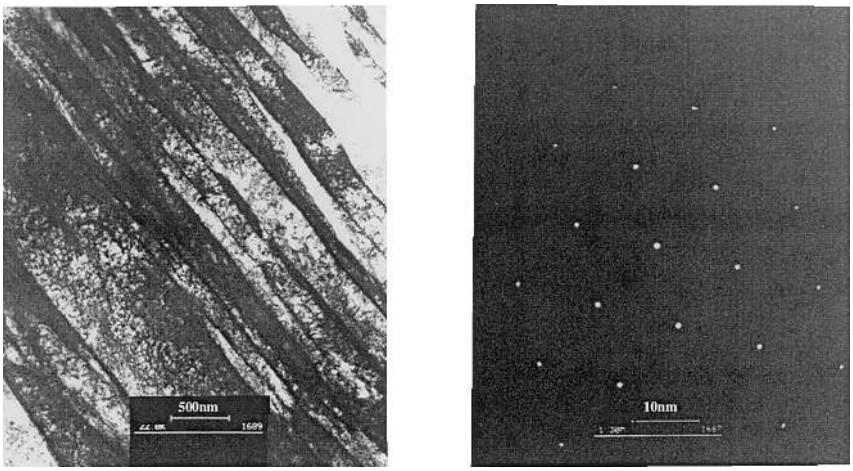

Fig. 2. Transmission electron micrograph of the interior of a block in lath martensitic steel. The bright-field micrograph shows a refined, sub-micron lath size. The diffraction pattern shows the laths are crystallographically almost identical, that is, they behave as a single crystal.

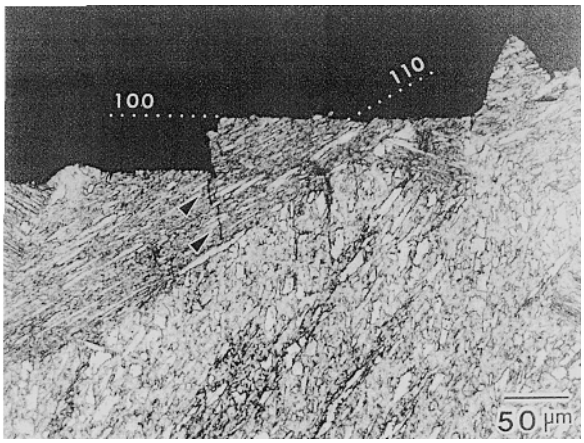

Fig. 3. Profile fractograph of cleavage fracture in as-quenched 9Ni steel. The cleavage facets cross laths, branch at packet boundaries and prior austenite grain boundaries.

tains a diffraction pattern that includes a number of adjacent laths within a block (in the steel shown, the block and packet sizes are the same). The diffraction pattern shows that the block is, essentially, a single crystal. The lath boundaries are low-angle boundaries that do not impose significant crystallographic discontinuities. Since the lath boundaries tend to lie parallel to {110}, the laths share common {100} planes that cut through the boundaries.

The practical implication of lath alignment within a block is illustrated in **Fig. 3**, which is a profile SEM fractograph of cleavage fracture below the ductile–brittle transition temperature of a large-grain lath martensitic steel. The steel is cleaved along {100} planes that cross many laths within a packet. The crack branches at packet boundaries where the orientation of the {100} planes changes.

A property of major concern in structural steels is the ductile–brittle transition temperature, T_B.[24,25] The connection between T_B and the cleavage fracture stress can be understood on the basis of a model that was originally suggested by the Russian physicist, Yoffee, in the early 20th century. The modern version can be stated as follows (**Fig. 4**). The peak tensile stress in the process zone of a crack tip in an elastic–plastic material, σ_T, scales with the yield

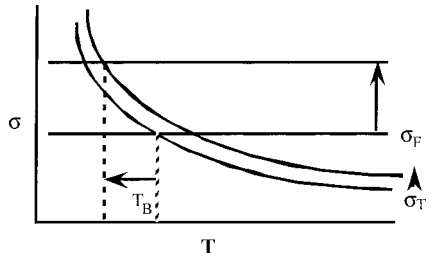

Fig. 4. The Yoffee diagram. The Yoffee model: the duictile–brittle transition occurs when the crack-tip stress (σ_T) exceeds the brittel fracture stress (σ_F). Redfining the grain size raises both σ_F and σ_T, but the effect on σ_F is ordinarily larger, with the result that T_B decreases.

strength, σ_y, and is of the order of $(3–5)\sigma_y$. It follows that this stress increases as the temperature drops. Assuming that the brittle fracture mode is cleavage, then so long as σ_T is below σ_F, the crack tip material yields before cleavage and the fracture is ductile. But in a typical ferritic or martensitic steel the thermal increment in σ_y has the consequence that decreasing temperature eventually raises σ_T above σ_F. When this happens, the material becomes liable to brittle fracture. The ductile–brittle transition occurs at a temperature close to the crossover point.

As illustrated in Fig. 4, the most direct way to decrease T_B is to raise the brittle fracture stress. Grain refinement is an effective way to do this. However, grain refinement also raises the yield stress. If we assume that the increase in the effective yield strength on decreasing temperature is approximately linear, with slope $(d\sigma/dT)$, then Eqs. (1) and (2) can be combined[5] to give Eq. (3), with the Hall–Petch coefficient,

$$K_B=\left[\frac{d\sigma}{dT}\right]^{-1}(K_f-K_y) \quad \text{.....(5)}$$

Given Eq. (1), the Hall–Petch relation for T_B can be re-written

$$T_B=T_0-\left[\frac{K_B}{K_y}\right](\sigma_y-\sigma_0) \quad \text{.....(6)}$$

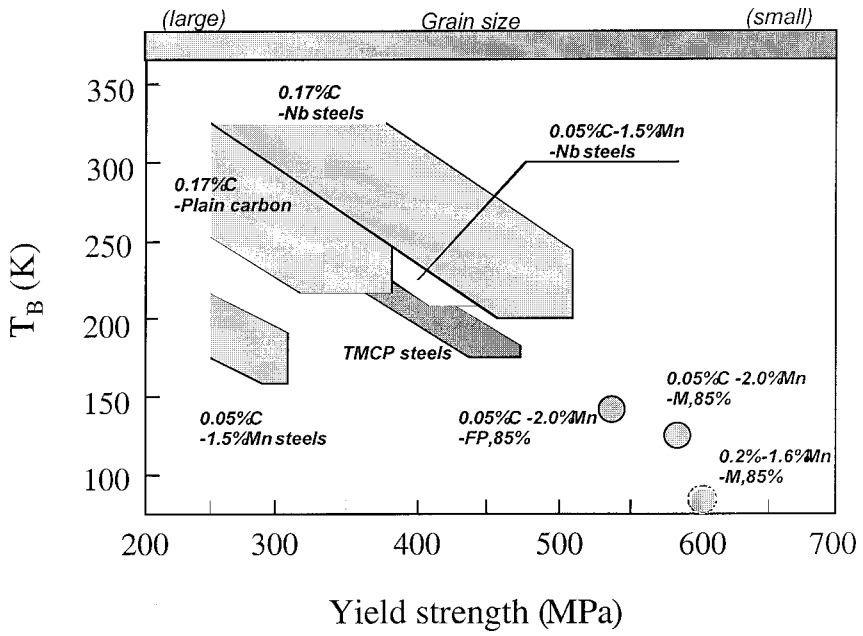

Fig. 5. Compilation of data showing the generally linear decrease in the ductile–brittle transition temperature with strength olbtained by grain refinement. Plot courtesy of Nagai,[26] includes data from Pickering[27] and Hanamura *et al.*[28]

When K_f is greater than K_y, as it is in every case known to us, T_B decreases as the grain size is refined and, therefore, decreases as the yield strength rises. A linear relation like that predicted in Eq. (6) is often found in carbon steels. **Figure 5** is a compilation of data that illustrates this behavior.[26–28]

To maximize the decrease in T_B with σ_y, Eqs. (5) and (6) suggest that the Hall–Petch coefficient for fracture, K_f, should be maximized while the coefficient for strength, K_y, should be minimized. Since K_f depends on the misorientation of {100} planes while K_y depends on the misorientation of {110} planes, it should be possible to accomplish this by controlling the crystallography of the refined grains.

2.4. The Effective Grain Size for Hydrogen Embrittlement

Hydrogen embrittlement appears to be a boundary phenomenon in ferritic or martensitic steels. Ordinarily, the hydrogen-induced fracture separates prior austenite grain boundaries.[29–34] In clean or gettered lath martensitic steels the hydrogen resistance is relatively good, and the fracture mode is transgranular.[31] A closer examination shows, however, that even in this case the fracture is primarily interfacial, along martensite lath boundaries (**Fig. 6**).

If the fracture is along grain or lath boundaries then the effective grain size is the length of semi-planar boundary segments. In lath martensitic steels the boundaries extend across the packet, so the effective grain size is the packet size. To overcome hydrogen embrittlement, it is necessary to refine the packet size to the optimal degree. However, as we have noted, the thermomechanical processes that are most effective in grain refinement lead to very high strength and very low ductility when the grain size drops below about 2 μm. To produce an alloy that maximizes hydrogen resistance while retaining good ductility, one would like to avoid excessive strength. To accomplish this, it is useful to minimize K_y.

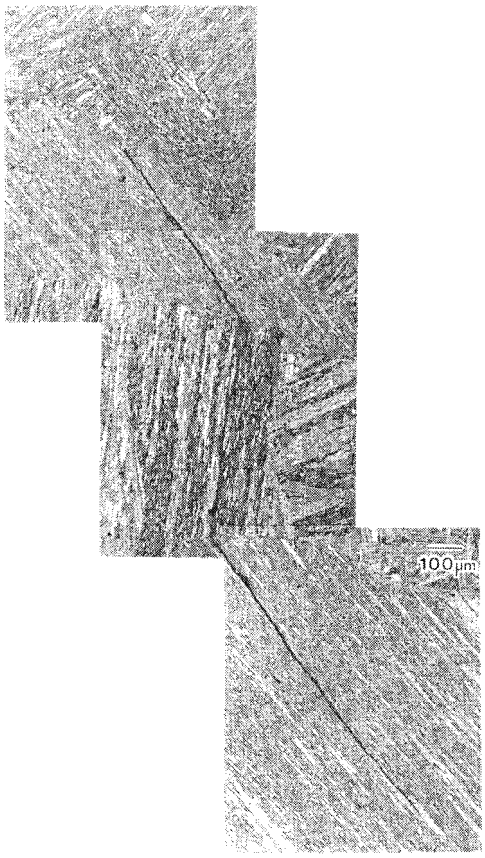

Fig. 6. Hydrogen-induced cracking of lath martensite in lath martensitic steel (6Ni). The cracks propagate across packets along lath boundaries, branching at packet boundaries.

The above discussion suggests that the three properties of interest, the strength, brittle transition and hydrogen resistance, have three different measures of the effective grain size. In a random polycrystal, these measures of grain size

are roughly the same. But in a crystallographically coherent transformation they may be very different.

3. Coherent Transformations in Steel

3.1. Crystallography of Coherent Transformations

As is well known, a coherent transformation from fcc austenite to bcc ferrite (or martensite) is accomplished by the "Bain strain", in which the austenite is compressed along one {100} direction and expanded in the perpendicular plane to achieve a bcc structure. Since there are three choices for the compressed {100} axis, a given fcc crystal can produce three distinct "Bain variants' of the bcc product.

However, the Bain strain is difficult to accomplish in a continuous transformation since it does not provide a coherent interface between the austenite and ferrite phases. To create a coherent interface between the close-packed {111} plane of fcc and the closest-packed {110} plane of bcc it is necessary to modify the Bain strain by rotating the bcc crystal and adding a small shear. The two planes can then be fit in either of two convenient ways, which are illustrated in **Fig. 7**. In this figure we assume $(111)_\gamma \| (011)_\alpha$ and choose the $[\bar{1}10]_\gamma$ direction as the reference. The two-dimensional configuration of the $(011)_\alpha$ plane is a face-centered rectangle bounded by the $[100]_\alpha$ and $[01\bar{1}]_\alpha$ directions. There are three ways to "almost" fit this rectangle onto the face-centered hexagonal configuration of atoms in the $(111)_\gamma$ plane so that the $[\bar{1}10]_\gamma$ direction is preserved.

The arrangement that is the simplest, physically, matches the close-packed directions in the two crystals by setting $[11\bar{1}]_\alpha \| [\bar{1}10]_\gamma$ (Fig. 7(a)) The $[100]_\alpha$ and $[01\bar{1}]_\alpha$ directions that define the bcc cell must then be slightly distorted to fit the fcc cell. This correspondence defines the Kurdumov–Sachs (KS) orientation relation. As shown in the figure, for each $[\bar{1}10]_\gamma$ reference direction there are two ways to make this correspondence, yielding two, twin-related KS variants.

The second simple crystallographic arrangement sets $[001]_\alpha \| [\bar{1}10]_\gamma$, as in Fig. 7(b). In this case the close-packed $[11\bar{1}]_\alpha$ direction must be distorted slightly to achieve correspondence. The result is the Nishiyama–Wasserman (NW) relation.

There are three independent ways to choose the $\langle 110 \rangle_\gamma$ direction in each $\{111\}_\gamma$ plane, and four independent ways to choose the $\{111\}_\gamma$ plane. Since each combination of

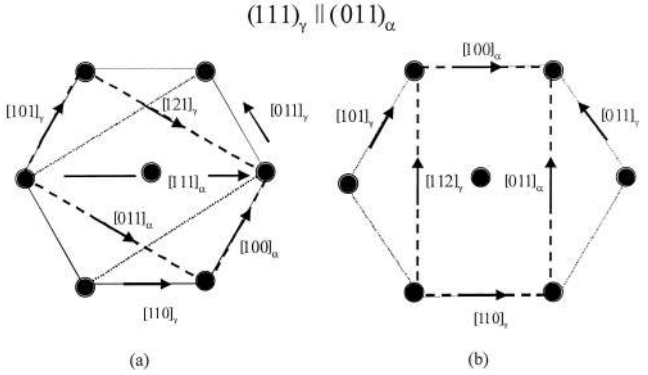

Fig. 7. Diagram showing the KS (a) and NW (b) correspondences for the $[110]_\gamma$ direction in the $(111)_\gamma$ plane. The twinned KS variant is also indicated in (a).

$\langle 110 \rangle_\gamma$ and $\{111\}_\gamma$ defines one NW variant and 2 KS variants, there are 36 distinguishable variants associated with a given coherent $\gamma \rightarrow \alpha$ transformation: 24 KS variants and 12 NW variants. The large number of KS and NW variants that are possible outcomes of the coherent transformation of a single austenite grain suggests that a coherent transformation is an automatic mechanism of grain refinement. But this apparent crystallographic complexity is deceptive, for two reasons.

3.1.1. Bain Variants

The first reason becomes apparent when we examine the transformation tensors that connect the austenite to a given variant of martensite. There are two relevant tensors. The first, **T**, is the overall transformation matrix that generates the principal axes of the bcc crystal from those of the parent fcc. It is the product of a deformation and a rotation. The deformation sets the transformation strain, **E**, that must be applied to the fcc crystal to create the unrotated bcc. While the transformation matrix is complex, the transformation strain is simple, and deviates only slightly from the Bain strain.

For example, the transformation matrices and transformation strains for a high-nickel steel are given by Guo.[35] Assuming the interface correspondence, $(111)_\gamma \| (011)_\alpha$, and using the fcc axes as the reference axes, the KS variant with $[\bar{1}10]_\gamma \| [11\bar{1}]_\alpha$ has

$$\mathbf{T}=\begin{bmatrix} 0.789 & -0.194 & -0.074 \\ -0.134 & 1.117 & -0.074 \\ 0.060 & 0.060 & 0.13 \end{bmatrix} \quad \text{.....(7)}$$

$$\mathbf{E}=\begin{bmatrix} -0.197 & 0.0002 & -0.0001 \\ 0.0002 & 0.135 & -0.0002 \\ -0.0001 & -0.0002 & 0.135 \end{bmatrix}$$

Note that the strain tensor is almost tetragonal. It is dominated by the Bain strain which, in this case, has its tetragonal axis in the *x*-direction (in an *x*, *y*, *z* labeling of the cubic axes). The transformation and strain tensors for the twinned KS variant and the NW variant associated with the same $\langle 110 \rangle_\gamma$, $\{111\}_\gamma$ set are very similar, with the difference that the twinned KS has its principal strain along the *y*-axis while the NW variant has its principle strain along *z*.[35] Thus, the three variants associated with a given $\langle 110 \rangle_\gamma$, $\{111\}_\gamma$ set correspond to the three possible variants of the Bain strain (the Bain variants).

The transformation and strain tensors of the 33 variants that are associated with the other 11 choices of $\langle 110 \rangle_\gamma$ and $\{111\}_\gamma$ can be found from these by applying the appropriate rotation matrices. The transformation strain tensors all have the same qualitative properties: the transformation strains are dominated by the Bain strain, and the three variants associated with each $\langle 110 \rangle_\gamma$, $\{111\}_\gamma$ set include two KS relations in twin orientation plus one NW relation, representing the three Bain variants. The precise numerical values of the elements of the tensors given in Eq. (7) depend on the lattice constants of the steel and, hence, on its pecise composition. But the qualitative features of these tensors are general.

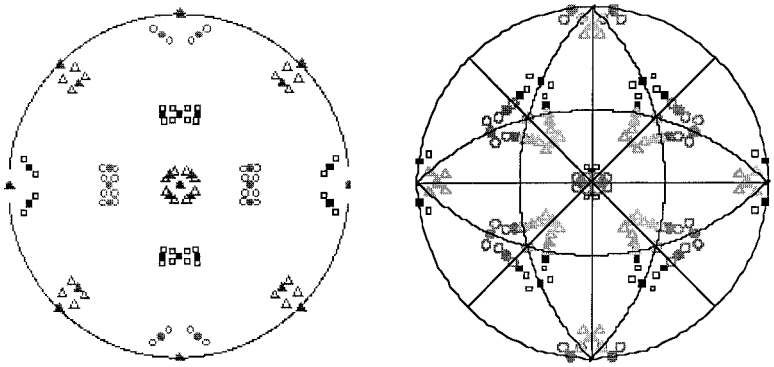

(a) (b)

Fig. 8. Stereographic projections of the (a) {100} and (b) {110} pole figures for the KS and NW variants of martensite derived from a single crystal of austenite. The open symbols are KS variants; the closed symbols are NW variants. The circles, squares and triangles denote the *x*, *y* and *z* Bain variants, respectively. Note that Bain variants are clearly separated in the {100} pole figure, but are contiguous in the {110} pole figure.

It follows that the 36 KS and NW variants of the coherent transformation divide into 3 sets of 8. Each set contains all variants that are derived from the same Bain variant, and differ very little from one another. In assessing the grain refinement that is achieved by a coherent transformation, it is important to focus on the different Bain variants that are produced, recognizing that there are only 3 of them.

On the other hand, there is a strong thermodynamic tendency toward multivariant transformations. The Bain strain changes both the shape and volume of the region it transforms, and, hence, severely distorts its surroundings. Two different Bain variants can join together to form a plate with an invariant plane. This possibility is the basis of the "crystallographic theory" of plate martensite,[36] and helps to explain the alternate-variant structure of "LQ"-treated lath martensitic steel.[35,37] Three variants can join together to produce a product that changes the volume only, significantly reducing the strain energy of a transformed grain that is constrained by its surroundings. This behavior promotes the formation of structures like that shown in Fig. 1, where prior austenite grains are subdivided into packets and blocks that represent multiple Bain variants. It follows that martensitic transformations ordinarily do provide grain refinement to the extent that this is accomplished by dividing prior austenite grains into multiple Bain variants.

3.1.2. Misorientations between Bain Variants

The extent to which transformation into a mixture of Bain variants refines the effective grain size depends on the misorientation of the critical crystallographic planes across the inter-variant boundaries. The possible misorientations of the {100} and {110} planes are illustrated in the pole figures shown in **Fig. 8**. As expected, the KS and NW variants that are derived from the same Bain variant cluster closely together in both pole figures. However, the misorientations between Bain variants are qualitatively different. In the {100} pole figure, Fig. 8(a), the clusters that mark different Bain variants are distinctly separated; {100} planes are always significantly misoriented across boundaries between different Bain variants. In the {110} pole figure, Fig. 8(b), the clusters that correspond to different Bain variants are close to one another, and almost overlap. It follows that inter-variant boundaries do not necessarily produce significant misorientations of {110} planes.

We infer that a coherent transformation into multiple Bain variants is an effective means for refining the grain size against cleavage, but should be less effective than random nucleation in refining the grain size for strength.

3.2. Examples of Coherent Transformations

Crystallographic coherence is a well-known feature of martensitic and Bainitic transformations. There is, moreover, an accumulating body of evidence that other mechanisms of the $\gamma \rightarrow \alpha$ transition are also coherent as well. The KS relationship has been identified in diffusional $\gamma \rightarrow \alpha$ transformations by using retained austenite,[14,15] transformed martensite[16] or deformation texture[11–13] as a crystallographic reference. More recently, we[17,18] have developed a systematic numerical technique to determine whether groups of ferrite grains are coherently related to the same parent austenite. This technique makes it possible to explore coherent relationships in low-carbon steels that transform completely to ferrite.

3.2.1. Martensitic Transformations

The structure of a typical lath martensitic steel is shown in Fig. 1. Prior austenite grains are divided into single-variant packets, or blocks. Multivariant structures within a single prior austenite grain minimize the overall elastic energy of the transformation.

A slightly different use of the coherent transformation is illustrated in **Fig. 9**, which shows how multivariant transformations can be used to refine grain size by breaking up lath alignment within a packet.[25,35,37] The steel shown in the transmission electron micrograph is "9Ni" steel that has been given an "LQ" treatment: an intercritical anneal (L) followed by an austenite reversion and quench (Q). The intercritical anneal creates a "dual phase" structure in which laths of high-Ni fresh martensite alternate with laths of relatively low-Ni well-tempered martensite. The Ni segregation is preserved when the packet is reverted to austenite, and has the consequence that its re-transformation to martensite occurs in two steps. The low-Ni material transforms first to a KS-related martensite. The high-Ni material then transforms under the constraint imposed by this

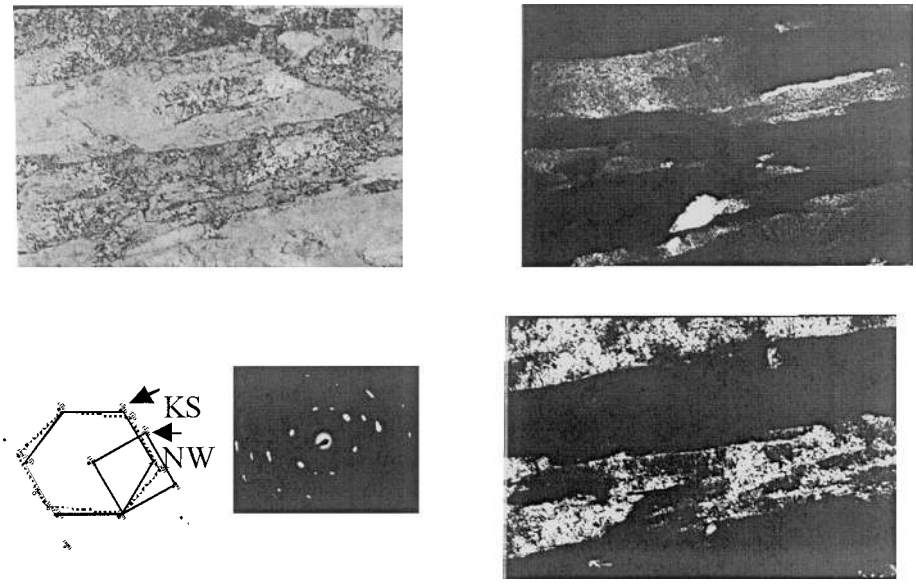

Fig. 9. TEM micrographs of 9Ni steel in the "NLQ" condition (1 423 K, 18 h for normalization (N); 963 K, 1h for intercritical annealing (L); 1 093 K, 1h, oil quenched (Q); 77 K, 1 h for chilling). Local diffraction pattern indicates two variants within the same martensite packet, which alternate as shown in the two dark field micrographs on the right.

martensite. To minimize elastic energy, it transforms into an NW-related martensite with a different Bain variant.[35] The result is the structure shown in the figure, in which two different Bain variants form alternate laths in a packet. Since {100} cleavage planes have large-angle deviations at the lath boundaries, this structure is highly resistant to cleavage fracture.

3.2.2. Acicular Ferrite Nucleation from an Oxide Inclusion

A somewhat more surprising example of coherent transformation is presented in **Fig. 10**, which shows the crystallography of acicular ferrite formed at an oxide inclusion. This particular example appeared in the heat-affected zone of a weldment in a steel that had been "salted" with oxide particles.[38] These particles are intended to maintain fine grain size in the heat-affected zone by providing a dense array of ferrite nucleation sites for retransformation of the austenite in the HAZ.

As shown in the figure, there are several ferrite grains around the oxide particle. All of them are coherently related to the same parent austenite. All three Bain variants appear, presumably to minimize the overall shape strain of the transformation.

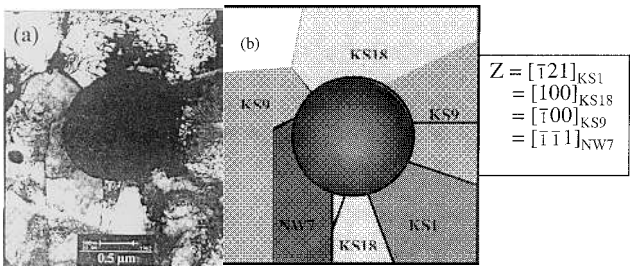

Fig. 10. Analysis of acicular ferrite nucleated from an oxide inclusion in the heat-affected zone of a weldment (Lee, Guo and Morris[17]). (a) Bright-field TEM. (b) Separation into crystallographically distinct ferrite grains. The ferrite grains are coherently related to the same parent austenite. Variants KS9 and KS18 are examples of one Bain variant, KS1 and NW7 are examples of the other two (original data from Lee *et al.*[38]).

3.2.3. Thermomechanical Processing

The thermomechanical processes that are currently being developed to produce ultrafine grained steels use deformation just above the transformation temperature on cooling (Ar_3) to introduce ferrite by strain-induced dynamic transformation (SIDT). Metallographic analysis of the transformation[39] suggests that the SIDT ferrite forms primarily along prior austenite grain boundaries, with the residual material in the grain interior transforming thermally on subsequent cooling. The thermomechanical process can be simulated by laboratory tests done in a test machine of the "Gleeble" type. For example, **Fig. 11** shows the fine-grained microstructure of a sample of 0.15C–0.25Si–1.1Mn

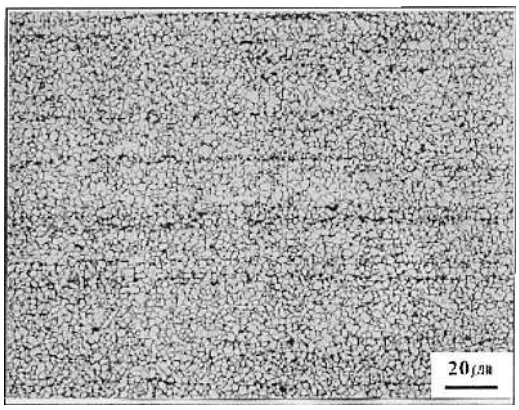

Fig. 11. Optical micrograph of 0.15C–0.25Si–1.1Mn steel that was thermally processed as follows: austenitization at 1 173 K, cooling to 1 048 K at 10 K/sec, 80% deformation at 1 048 K, cooling at 10 K/sec. The microstructure is a mixture of strain-induced (SIDT) and thermal ferrite.

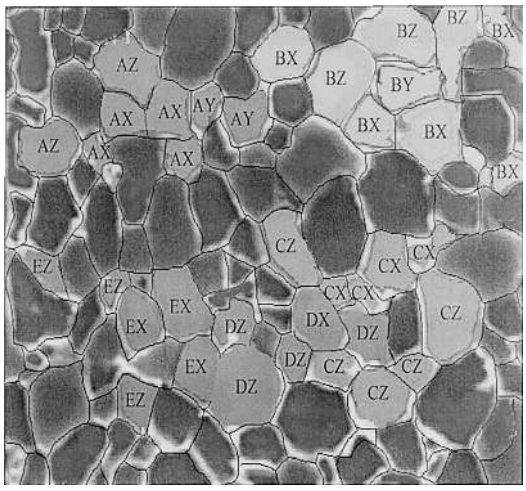

Fig. 12. Orientation analysis (EBSD) of a group of grains taken from the micrograph shown in Fig. 11. The labeled grains are sets that are coherently related to the same parent austenite. The letters A–E denote five different coherent sets. The letters X, Y, Z denote the three distinct Bain variants.

steel that was heated at 1 173 K, deformed 80% at 1 048 K (just above Ar_3), cooled at 10 K/s to 823 K, and then cooled at 1 K/s to ambient temperature.

Figure 12 shows the subsets of the grains in Fig. 11 that are coherently related to the same parent austenite. The coherent grains are labeled with upper case letters (A, B, C ...) to distinguish different sets (different orientations of the parent austenite) and lower case letters (*x*, *y z*) to designate the different Bain variants. The coherent grains appear to form sets that are separated by layers of incoherent grains. Five distinct sets appear in the metallographic section that was analyzed. The sets appear to be flattened and elongated, in keeping with their derivation from deformed γ-grains, and contain two or more Bain variants. In the regions between the coherent regions, no more than two or three grains can be assigned coherent orientation relationships with a given austenite.

Comparing these results with the metallographic analysis by Choo and coworkers[39] suggests that the clusters of coherent grains are thermally transformed austenite in the grain interiors, while the surrounding sets of incoherent grains are the "SIDT" ferrite in the prior austenite grain boundaries. While further research is needed, it appears that the thermal transformation is largely coherent while the dynamic transformation is not.

4. Mechanical Consequences of Coherent Transformations

The general considerations we have set out above suggest that grain refinement to increase strength is best done with incoherent transformations, but it is preferable to use multivariant coherent transformations to control brittle fracture or resistance to hydrogen embrittlement.

4.1. Strength

The strengthening effect of thermomechanical processes that refine the grain size of carbon and low alloy steels is well known. Recent research[1–4] suggests, moreover, that dynamic transformation from γ to α is particularly effective. Data like that shown in Fig. 12 suggest a probable reason; dynamic transformation promotes incoherent $\gamma \rightarrow \alpha$ transformation, which efficiently refines the coherence length along {110} slip planes.

On the other hand, grain refinement by coherent transformations is often quite ineffective in raising the strength. Cyclic martensitic transformations that achieve ultrafine grain size with respect to fracture have very little effect on the strength, particularly in low-carbon or interstitial-free steels. For example, ultrafine grained (8–12)Ni,[40–43] 5Mn[44] and Ni–Mo–Cr–Co steels[35,37] have strengths almost identical to those in the unrefined condition. In these alloys it has been necessary to harden with other mechanisms, such as dislocated martensite[40–44] or precipitation hardening.[35,37]

4.2. Cleavage Fracture

The efficiency with which coherent transformations lower the ductile–brittle transition temperature is well documented,[24] particularly in lath martensitic steels. Grain refinement by controlled, cyclic martensitic transformations has been used to create steels that have good strength/toughness combinations at temperatures as low as 4 K,[40,42] and to develop multipass welding procedures that permit the use of ferritic filler metals in welding ferritic cryogenic steels.[45,46]

In fact, even the conventional ferritic cryogenic steels, tempered "9Ni" and "6Ni" steels, are, indirectly, refined in this way. These steels are given controlled tempering treatments to introduce retained austenite along lath boundaries. However, this austenite is mechanically unstable, and transforms under load prior to fracture.[24,43,47] The usual transformation product is a Bain variant that differs from that of the surrounding packet,[24,43] disrupting the cleavage planes.

High-Ni lath martensitic steels combine good strength with high toughness and a low ductile–brittle transition temperature. However, the strength is almost entirely due to the highly dislocated lath martensite substructure. As noted above, the refinement of martensite packets contributes very little to the strength.

4.3. Hydrogen Embrittlement

Given that hydrogen embrittlement is essentially a boundary phenomenon, it is best overcome by refining to ultrafine grain size. However, this must be done in a way that does not increase strength to a level that destroys ductility. It follows that grain refinement by coherent transformations is an attractive path, since it creates the possibility of reaching ultrafine effective grain size without overstrengthening.

Perhaps the simplest method for refining the coherent crack length along hydrogen-sensitive boundaries is to simply serrate the boundaries. A serrated boundary has a small coherent crack length whether or not the grain interiors are effectively refined. A promising recent use of this technique is in work by Tsuzaki and coworkers,[48,49] who severely ausformed high-strength steel prior to coherent transformation. The severe deformation during ausforming serrates the prior austenite grain boundaries and breaks up boundary carbide films, producing a steel that is hydrogen-resistant even through the prior austenite grain size remains relatively coarse.

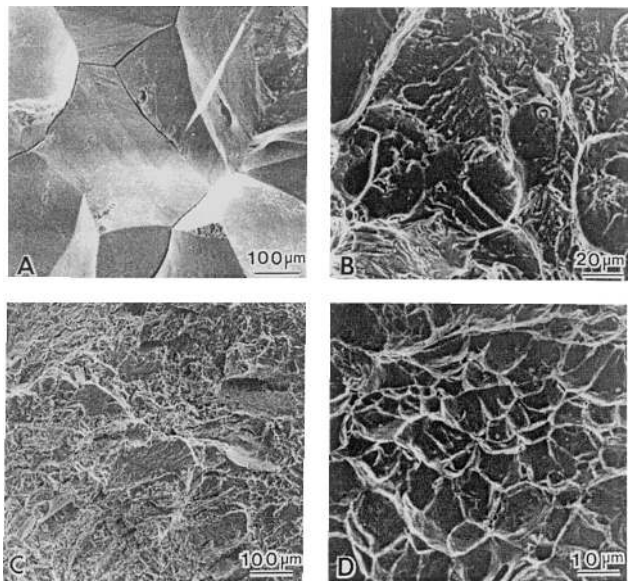

Fig. 13. Scanning electron fractographs of 12Ni–0.25Ti steel broken after hydrogen charging after various heat treatments. (A) Quenched and tempered at 723 K for 300 h.; brittle intergranular fracture. (B) As quenched; brittle transgranular fracture. (C) Rapid ("spike") reversion to austenite; primarily ductile fracture. (D) Double "spike" reversion to austenite, then tempered at 723 K for 300 h.; fully ductile fracture.

Other researchers have used rapid thermal cycling treatments to produce martensitic or coherent ferritic steels with ultrafine block sizes. Research in our laboratory some years ago[10,25.30] showed that (6–12)Ni steels could be made virtually immune to hydrogen embrittlement by a two-step rapid reversion treatment ($\alpha' \rightarrow \gamma \rightarrow \alpha'$) that produces a coherent product with a submicron "packet" size. **Figure 13** illustrates the effectiveness of this treatment for 6Ni steel. The 6Ni steel is a dislocated martensitic steel with a high strength, which increases only slightly during grain refinement by cyclic transformation. Similar rapid reversion treatments have recently been used by Dong and co-workers[50,51] to dramatically improve the delayed fracture resistance of high strength bolt steels made of a modified 4140 alloy.

An effective modification of this cycling procedure has been proposed by Yokota, *et al*.,[22,52] who used severe mechanical deformation just below the ($\alpha' \rightarrow \gamma$) reversion temperature of a 9Ni–0.3C steel to trigger a partial reverse transformation by adiabatic heating. When this treatment is followed by a rapid ($\alpha \rightarrow \gamma \rightarrow \alpha$) reversion cycle, the result is an ultrafine-grained product with a promising combination of strength and cold-cracking resistance.

5. Conclusion

Three properties that often important in structural steels, strength, ductile–brittle transition and hydrogen resistance, are all strongly influenced by grain size. However, the mechanisms that determine these properties differ, with the consequence that each depends on a slightly different measure of the effective grain size. When the grains are randomly oriented and the grain boundaries are smooth, all measures of the effective grain size are roughly the same. However, transformations in steel are often crystallographically coherent. The coherent transformation produces a martensitic or ferritic product that has a KS or NW relation to the parent austenite. The 24 KS variants and 12 NW variants divide into three sets of eight, corresponding to the three Bain variants of the fcc→bcc transformation. Grain, packet or block boundaries that separate different Bain variants have significant misorientations of the {100} cleavage planes, but may have only slight misorientations of the {110} slip planes. It follows that grain refinement through coherent transformation is very effective in improving resistance to cleavage fracture and, if the boundary facets are small, to hydrogen embrittlement, but is often ineffective in increasing strength. For this reason, grain refinement for increased strength is best done with incoherent transformations (such as the strain-induced ferrite transformation) while grain refinement for low-temperature toughness or hydrogen resistance is best done with coherent transformations that refine the effective grain size without the overstrengthening that leads to unacceptably low ductility.

Acknowledgements

This work was supported by the Director, Office of Energy Research, Office of Basic Energy Science, Materials Science Division of the U.S. Department of Energy, under contract No. DE-AC03-76SF00098, and was also supported by a grant from Pohang Iron and Steel (POSCO).

REFERENCES

1) Ultrafine Grained Steels, ed. by S. Takaki and T. Maki, ISIJ, Tokyo, (2001).
2) NG Steel '2001, The Chinese Society for Metals, Beijing, (2001).
3) The Development of High Performance Structural Steels for 21st Century (Hipers-21), Pohang Iron and Steel Company and Korean Institute for Metals, Pohang, (2002).
4) Proc. 1st Int. Conf. on Advanced Structural Steels, NIMS, Tsukuba, (2002).
5) J. W. Morris, Jr.: Ultrafine Grained Steels, ed. by S. Takaki and T. Maki, ISIJ, Tokyo, (2001), 34.
6) R. Marder and G. Krauss: *Trans. Am. Soc. Met.*, **62** (1969), 957.
7) T. Maki, K. Tsuzaki and I. Tamura: *Trans. Iron Steel Inst. Jpn.*, **20** (1980), 209.
8) T. Maki: NG Steel '2001, The Chinese Society for Metals, Beijing, (2001), 27.
9) J. W. Morris, Jr., J. I. Kim and C. K. Syn: Advances in Metal Processing, ed. by J. Burk, R. Mehrabian and V. Weiss, Plenum Press, (1981), 173.
10) H. J. Kim, Y. H. Kim and J. W. Morris, Jr.: *ISIJ Int*., **38** (1998), 1277.
11) R. K. Ray and J. J. Jonas: *Int. Mater. Rev.*, **35**, (1990), 1.
12) P. J. Hurley, P. D. Hodgson and B. C. Muddle: *Scr. Mater*., **40** (1999), 433.
13) P. J. Hurley and P. D. Hodgson: *Mater. Sci. Eng. (A)*, **302** (2001), 206.
14) H. Y. Yasuda, T. Sakada and Y. Umakoshi: *Acta Mater*., **47** (1999), 1923.
15) T. Furuhara and T. Maki: *Mater. Sci. Eng*. (A), **312** (2001), 145.
16) D. W. Suh, J. Y. Cho, J. H. Kang, K. H. Oh and H. C. Lee: Ultrafine Grained Steels, ed. by S. Takaki and T. Maki, ISIJ, Tokyo, (2001), 214.
17) C. S. Lee, Z. Guo, D. H. Seo and J. W. Morris, Jr.: The Development of High Performance Structural Steels for 21st Century (Hipers-21), Pohang Iron and Steel Company and Korean Institute for Metals, Pohang, (2002), 139.
18) C. S. Lee and J. W. Morris, Jr.: unpublished research.
19) N. Tsuji, Y. Ito, R. Ueji, Y. Koizumi and Y. Sato: Ultrafine Grained Steels, ed. by S. Takaki and T. Maki, ISIJ, Tokyo, (2001), 256.

20) S. Takaki, K. Kawasaki and Y. Kimura: Ultrafine Grained Materials, ed. by R. S. Mishra *et al*., The Metallurgical Society, Warrendale, PA, (2000), 247.
21) S. Takaki: Ultrafine Grained Steels, ed. by S. Takaki and T. Maki, ISIJ, Tokyo, (2001), 42.
22) M. Niikura, T. Yokota, K. Sato, Y. Shirota, S. Hinotani, Y. Adachi, S. Namba, M. Fujioka and S. Aihara: NG Steel '2001, The Chinese Society for Metals, Beijing, (2001), 100.
23) W. Y. Choo: The Development of High Performance Structural Steels for 21st Century (Hipers-21), Pohang Iron and Steel Company and Korean Institute for Metals, Pohang, (2002), 1.
24) J. W. Morris, Jr., Z. Guo and C. R. Krenn: Heat Treating: Steel Heat Treating in the New Millennium, ed. by S. J. Midea and G. D. Pfaffmann, ASM, Metals Park, Ohio, (2000), 526.
25) J. W. Morris, Jr., Z. Guo, C. R. Krenn and Y. H. Kim: *ISIJ Int.*, **41** (2001), 599.
26) K. Nagai: National Institute for Materials Science (NIMS), Tsukuba, Japan, private communication, (2001).
27) F. B. Pickering: Physical Metallurgy and the Design of Steels, Applied Science Publishers, Ltd., London, (1978).
28) T. Hanamura, H. Nakajima, S. Torizuka, K. Tsuzaki and K. Nagai: *CAMP-ISIJ*, **12** (1999), 451.
29) C. J. McMahon: Hydrogen Effects in Metals, ed. by I. M. Bernstein and A. W. Thompson, TMS, Warrendale, PA, (1981), 219.
30) Y. H. Kim: PhD Thesis, Dept. Materials Science and Engineering, Univ. of California, Berkeley, (1985)
31) Y. H. Kim and J. W. Morris, Jr.: *Metall. Trans*., **14A** (1983), 1883.
32) Y. H. Kim, H. J. Kim and J. W. Morris, Jr.: *Metall. Trans*., **17A** (1986), 1157.
33) S. Yusa, T. Hara and K. Tsuzaki: *J. Jpn. Inst. Met*, **64** (2000), 1230.
34) Y. Weng, W. Hui and H. Dong: NG Steel '2001, The Chinese Society for Metals, Beijing, (2001), 62.
35) Z. Guo: PhD Thesis, Dept. Mat. Sci. and Eng., Univ. of California, Berkeley, (2001).
36) A. G. Khatchaturyan: Theory of Structural Transformations in Solids, J. Wiley, New York, (1983).
37) J. W. Morris, Jr., Z. Guo, K. Sato and T.-K. Lee: Ultrafine Grained Materials, ed. by R. S. Mishra, S. L. Semiatin, C. Suryanarayana, and N. N. Thadhanis, TMS, Warrendale, PA, (2000), 51.
38) T. K. Lee, H. J. Kim, B. Y. Kang and S. K. Hwang: *ISIJ Int*., **40** (2000), No. 12, 1260.
39) W. Y. Choo: NG Steel '2001, The Chinese Society for Metals, Beijing, (2001), 16.
40) S. Jin, J. W. Morris, Jr. and V. F. Zackay: *Metall. Trans*., **6A** (1975), 141.
41) S. Jin, S. K. Hwang and J. W. Morris, Jr.: *Metall. Trans*., **6A** (1975), 1721
42) H. J. Kim, H. Shin and J. W. Morris, Jr.: Proc. Int. Cryo. Mat. Conf., ed. by K. Tachikawa and A. Clark, Butterworths, London, (1983), 129.
43) J. I. Kim, C. K. Syn and J. W. Morris, Jr.: *Metall. Trans*., **14A** (1983), 93.
44) M. Niikura and J. W. Morris, Jr.: *Metall. Trans.*, **11A** (1980), 1531.
45) H. J. Kim and J. W. Morris, Jr.: *Welding J*., **62** (1983), 210.
46) Kobe Steel, Ltd., Welding Electrode Division, Tech. Report No. RDPD-7902, Oct., (1979).
47) C. K. Syn, B. Fultz and J. W. Morris, Jr.: *Metall. Trans*., **9A**, 1635 (1978).
48) S. Terazaki, S. Sakashita, S. Takagi, Y. Kimura and K. Tsuzaki: NG Steel '2001, The Chinese Society for Metals, Beijing, (2001), 239.
49) Y. Kimura, S. Takagi, S. Terasaki, T. Hara and K Tsuzaki: The Development of High Performance Structural Steels for 21st Century (Hipers-21), Pohang Iron and Steel Company and Korean Institute for Metals, Pohang, (2002), 89.
50) H. Dong: Ultrafine Grained Steels, ed. by S. Takaki and T. Maki, ISIJ, Tokyo, (2001), 18.
51) M. Wang, H. Dong, W. Hui, S. Chen and Y. Weng: The Development of High Performance Structural Steels for 21st Century (Hipers-21), Pohang Iron and Steel Company and Korean Institute for Metals, Pohang, (2002), 243.
52) T. Yokota, T. Shiraga, M. Niikura and K. Sato: Ultrafine Grained Materials, ed. by R. S. Mishra *et al*., The Metallurgical Society, Warrendale, PA, (2000), 267.